Chapter 5
Uncertainty propagation in Experimental Modal Analysis

Bart Peeters, Mahmoud El-Kafafy, Patrick Guillaume, and Herman Van der Auweraer

Abstract As all experimental procedures, Experimental Modal Analysis (EMA) is subject to a wide range of potential testing and processing errors. The modal identification methods are sensitive to these errors, yielding modal results which are uncertain up to certain error bounds. The question hence is what these error bounds on test data and modal parameters are. In this paper, the studied source of uncertainty is related to the variance (noise) on the Frequency Response Function (FRF) measurements. Under the H1 assumptions and in single-input cases, the FRF variances can be computed from the coherences and the FRFs. In multiple-input cases, some more measurement functions are required. Advanced system identification methods like the Maximum Likelihood Estimator (MLE) and PolyMAX Plus have the possibility to take the uncertainty on the measurement data into account and to propagate the data uncertainty to (modal) parameter uncertainty. This paper will review FRF variance estimation techniques, including some pragmatic approaches. The basic concepts of Maximum Likelihood Estimation and the calculation of confidence bounds will be discussed. Some typical structural testing and modal analysis cases will be used as illustration of the discussed concepts.

Keywords PolyMAX Plus • Uncertainty propagation • Maximum Likelihood Estimation • Experimental Modal Analysis

5.1 Introduction

The usefulness of structural dynamics test and analysis results for solving noise and vibration problems or for performing a design assessment or a design optimisation, depends largely on the confidence that one can have in these results. In other words, the results must be characteristic for the actual problem (and not be the result of testing artefacts) and the models must be representative for the actual behaviour of the investigated structure(s). Essentially, two types of problems are distinguished: (1) the test and modelling data are subject to experimentation and analysis errors and (2) the tested (or modelled) structure is not representative for the actual structure. A third (and often neglected) potential problem with the significance of the analysis results can originate from a violation of the assumptions used to model the structure. One of the most prominent examples is the effect of nonlinear structural behaviour on a linear (e.g. modal) model identification process.

The first problem is this of experimentation and analysis uncertainty. The "true" test result can in principle never be achieved. The level of the uncertainty associated with the test result is however not easy to quantify. A multitude of totally different causes may be at the origin of major bias and/or variance errors in the analysis. Adequate testing and analysis procedures may reduce (at least some of) these errors significantly, but a proper overall uncertainty quantification is hard to issue. Also in building numerical simulation models (e.g. based on the Finite Element approach), uncertainty is introduced by discretization effects, through imperfectly known material, geometry or loading parameters, or through uncertainty in the applicable model formulations.

The second problem is this of product variability, introducing changes in the structural dynamics characteristics because of differences in material, geometric, manufacturing or even operational use (loading, temperature . . .) parameters when

B. Peeters (✉) • H. Van der Auweraer
LMS International, Interleuvenlaan 68, 3001 Leuven, Belgium
e-mail: bart.peeters@lmsintl.com

M. El-Kafafy • P. Guillaume
Vrije Universiteit Brussel (VUB), Pleinlaan 2, 1050 Brussel, Belgium

H.S. Atamturktur et al. (eds.), *Model Validation and Uncertainty Quantification, Volume 3: Proceedings of the 32nd IMAC, A Conference and Exposition on Structural Dynamics, 2014*, Conference Proceedings of the Society for Experimental Mechanics Series, DOI 10.1007/978-3-319-04552-8_5,

compared to the "nominal" case. It is important to have at least an idea on the magnitude of these changes and their impact on the final product behaviour when assessing and optimising the design based on an "ideal" product model. While statistical product testing may reveal such performance spread, this is in general very hard to realize. The evaluation of the uncertainty of the product performance starting from uncertainty bounds on the model parameters is an alternative approach [1].

In [2], a stochastic model updating method is introduced. The idea is to propagate the uncertainty in the Test to uncertainty bounds on certain parameters of the Finite Element Model: the uncertain eigenfrequencies and mode shapes from the experimental modal analysis are utilised to identify model parameter means and covariance matrix. The application of stochastic model updating to an aerospace structure is discussed in [3].

Experimental Modal Analysis has evolved to a widely accepted methodology in the analysis and optimisation of the dynamic behaviour of mechanical and civil structures. Modal tests are a standard part of the analysis and refinement of physical prototypes or even operational structures. The modal model results are considered to be a deterministic system description, which can be used for multiple applications, ranging from a mere verification of the fulfilment of the design criteria, to the validation and updating of CAE models and the integration in hybrid system models. In reality, the modal results are just an estimation of the model parameters based on a series of input–output or output-only tests and hence subject to all related testing and modelling errors. These data errors can be just stochastic disturbances on the input/output data, but can also be caused by invalid model assumptions or data processing effects. Some of the main sources of errors are [1, 4, 5]:

- Sensor location and orientation errors.
- Test set-up loading and constraining effects.
- Sensor loading effects on the test structure.
- Sensor calibration and data conversion errors.
- Disturbance and distortion in the test data measurement chain.
- Signal processing errors.
- Model estimation errors.

In this paper, the studied source of uncertainty is related to the variance (noise) on the Frequency Response Function (FRF) measurements. Assuming that there are neither modelling nor non-linear distortion errors, the residual errors between the selected parametric model and the measured FRFs should be mainly due to the noise that polluted the measurement data (e.g. measurement noise, process noise, generator noise and digitization noise). Then, if the probability density function of the noise on the measured data is known, the Maximum Likelihood Estimator (MLE) can be constructed with the aim to maximize this probability function.

In Sect. 5.2, FRF variance estimation techniques will be reviewed including some pragmatic approaches. Advanced system identification methods like the Maximum Likelihood Estimator (MLE) and PolyMAX Plus have the possibility to take the uncertainty on the measurement data into account and to propagate the data uncertainty to (modal) parameter uncertainty. This is discussed in Sect. 5.3. Finally, in Sect. 5.4, some typical structural testing and modal analysis cases are illustrating the discussed concepts.

5.2 Estimation of FRF Variance

In this section, FRF and FRF variance estimation will be reviewed for the general multiple-input case. It is most common in experimental modal analysis (EMA) to use the so-called H1 estimator for calculating the FRFs. This estimator is consistent in case only output noise is present and can be written as:

$$[H] = \left[S_{yu}\right].[S_{uu}]^{-1} \tag{5.1}$$

with $[H(\omega)] \in \mathbb{C}^{N_o \times N_i}$ the FRF matrix of a system with N_i inputs and N_o outputs and consisting of elements H_{oi}, the FRF between output 'o' and input 'i'; $\left[S_{yu}\right] \in \mathbb{C}^{N_o \times N_i}$ the output–input cross spectrum matrix; $[S_{uu}] \in \mathbb{C}^{N_o \times N_i}$ the input spectrum matrix.

For the single-input case (we drop the sub-index 'i' in the following), the H1 FRF H_o and coherence function γ_o^2 can be written as:

$$H_o = \frac{S_{y_o u}}{S_{uu}}, \quad \gamma_o^2 = \frac{\left|S_{y_o u}\right|^2}{S_{uu} S_{y_o y_o}} \tag{5.2}$$

The coherence function is a value between 0 and 1, expressing the quality of the estimated FRF [6]. It can be shown [7] that under the H1 assumptions, and in the single-input case, the FRF variances can be computed from the coherences and the number of averaged data blocks used in the FRF and coherence calculations, N_{avg}, as follows:

$$\sigma^2_{H_o} = \frac{1}{N_{avg}} \left(\frac{1-\gamma^2_o}{\gamma^2_o} \right) |H_o|^2 \tag{5.3}$$

In the multiple-input case, some more measurement functions are needed. The multiple coherence function $m\gamma^2_o$ is the ratio of the part of the output spectrum that is a linear combination of all inputs, $S^{\text{predicted}}_{y_o y_o}$, and the output spectrum itself $S_{y_o y_o}$:

$$m\gamma^2_o = \frac{S^{\text{predicted}}_{y_o y_o}}{S_{y_o y_o}} = \frac{< H_o > [S_{uu}] \{H_o^H\}}{S_{y_o y_o}} \tag{5.4}$$

in which $< H_o > \in \mathbb{C}^{1 \times N_i}$ is the row of the FRF matrix Eq. (5.1) related to the output 'o'. The covariance matrix of the FRFs at output 'o' can be computed as:

$$C_{<H_o>} = \frac{1}{N_{avg}} \left(1 - m\gamma^2_o\right) S_{y_o y_o} . [S_{uu}]^{-1} \tag{5.5}$$

which can be considered as the MIMO extension of Eq. (5.3). The variance $\sigma^2_{H_{oi}}$ of H_{oi}, an individual element of the FRF matrix, can be found on the diagonal of the matrix $C_{<H_o>}$.

So to calculate the variances on the FRFs in case of multiple inputs, following quantities are needed: the number of averages, the multiple coherences, the output power spectra and the full input spectrum matrix Eq. (5.5). Unfortunately, not all these quantities are typically calculated and stored during a modal analysis test. Most often only FRFs and coherences are available. In the following we will introduce some pragmatic approaches to estimate the FRF variances in case some of the required quantities are missing.

Based on Eq. (5.4), it can be concluded that the output power spectra are not strictly needed: they can be substituted by:

$$S_{y_o y_o} = \frac{< H_o > [S_{uu}] \{H_o^H\}}{m\gamma^2_o} \tag{5.6}$$

In some cases, not the full input spectrum matrix is available, but only the input power spectra (i.e. its diagonal elements). If it is assumed that the inputs are uncorrelated, expression Eq. (5.5) can still be used, but with a diagonal input spectrum matrix. If no information on the inputs is available, a solution could be to assume that all inputs are uncorrelated and have equal power spectra. The diagonal elements of Eq. (5.5) can then be written as:

$$\sigma^2_{H_{oi}} = \frac{1}{N_{avg}} \left(\frac{1-m\gamma^2_o}{m\gamma^2_o} \right) \sum_{j=1}^{N_i} \left| H_{oj} \right|^2 \tag{5.7}$$

In which only the FRFs and the (multiple) coherences are required to estimate the FRF variance. This approach is based on the assumption that the inputs are uncorrelated and have equal power spectra. This is a quite common case in EMA: typically similar shaker types are used in multiple-input experiment and the drive signals (V) are often tuned to get similar input force spectra (N).

Finally, if no noise information is available (only FRFs, even no coherences), a residual error approach can be adopted. It estimates the noise on the FRFs by smoothing the residual errors between the measured FRFs and the estimated (synthesized) FRFs. These estimated FRFs are for instance obtained from the starting values of the MLE iterations (see Sect. 5.3). It is also possible to first perform some MLE iterations without including the variances, then calculating the residual error variances from the difference between data and MLE model, and finally perform some more MLE iterations with noise weighting. The advantage is that the residual error approach is also applicable to Operational Modal Analysis.

5.3 The Polymax Plus Method

In this section, the PolyMAX Plus method is briefly reviewed. More detailed explanations can be found in [8–11]. The PolyMAX Plus method is a frequency-domain modal parameter estimation method; i.e. it estimates the modal parameters using measured FRFs as primary data. It is well-known that the modal decomposition of an (acceleration over force) FRF matrix can be written as:

$$[H(\omega)] = \sum_{i=1}^{n} \frac{\{v_i\} < l_i^T >}{j\omega - \lambda_i} + \frac{\{v_i^*\} < l_i^H >}{j\omega - \lambda_i^*} + [LR] + (j\omega)^2 [UR] \tag{5.8}$$

where n is the number of complex conjugated mode pairs; $\bullet^*$ is the complex conjugate of a matrix; $\{v_i\} \in \mathbb{C}^{N_o}$ are the mode shapes; $< l_i^T > \in \mathbb{C}^{1 \times N_i}$ are the modal participation; and λ_i are the poles, which are related to the eigenfrequencies ω_i and damping ratios ξ_i as follows:

$$\lambda_i, \lambda_i^* = -\xi_i \omega_i \pm j\sqrt{1-\xi_i^2}\omega_i \tag{5.9}$$

The lower and upper residuals, $LR, UR \in \mathbb{R}^{N_o \times N_i}$, have been introduced to model the influence of the out-of-band modes in the considered frequency band.

A poly-reference method such as PolyMAX yields a set of poles and corresponding operational reference factors from the interpretation of the stabilization diagram. The mode shapes and the lower and upper residuals are then readily obtained by solving Eq. (5.8) in a linear least-squares sense. This second step is commonly called least-squares frequency-domain (LSFD) method.

5.3.1 First Stage: Maximum Likelihood Estimator

Assuming the measured FRFs to be uncorrelated, the maximum likelihood cost function reduces to [12]:

$$\ell^{\mathrm{ML}}(\theta) = \sum_{o=1}^{N_o} \sum_{i=1}^{N_i} \sum_{k=1}^{N_f} \frac{\left| H_{oi}^{ML}(\omega_k, \theta) - H_{oi}(\omega_k) \right|^2}{\sigma_{H_{oi}}^2(\omega_k)} \tag{5.10}$$

where $H_{oi}(\omega_k)$ and $\sigma_{H_{oi}}(\omega_k)$ are the measured FRF and its standard deviation at frequency ω_k. The summations run over the number of outputs N_o, the number of inputs N_i and the number of frequency lines N_f. The FRF model $H_{oi}^{ML}(\omega_k,\theta)$ is a common-denominator model, where the numerator and denominator polynomials are expressed in the z-domain. The polynomial coefficients θ are estimated by minimizing Eq. (5.10). This can be done by means of a Gauss-Newton optimization algorithm, which takes advantage of the quadratic form of the cost function. The Levenberg-Marquardt algorithm is used to ensure a continuous decrease of the cost function during the iterations.

Alternatively, the MLE-like logarithmic estimator minimizes the following cost function:

$$\ell^{\text{LOG-ML}}(\theta) = \sum_{o=1}^{N_o} \sum_{i=1}^{N_i} \sum_{k=1}^{N_f} \frac{\left| \log\left(H_{oi}^{\mathrm{ML}}(\omega_k, \theta) / H_{oi}(\omega_k) \right) \right|^2}{\sigma_{H_{oi}}^2(\omega_k) / \left| H_{oi}(\omega_k) \right|^2} \tag{5.11}$$

This logarithmic estimator has nearly MLE properties and is more robust against the noise assumptions made as well as outliers, and can handle measurements with a large dynamic range. More details on the algorithm can be found in [9] and the references cited therein.

It is important to note that the MLE formulation requires not only the FRF measurements, but also estimates of their standard deviation. It has been explained in Sect. 5.2 how these could be obtained.

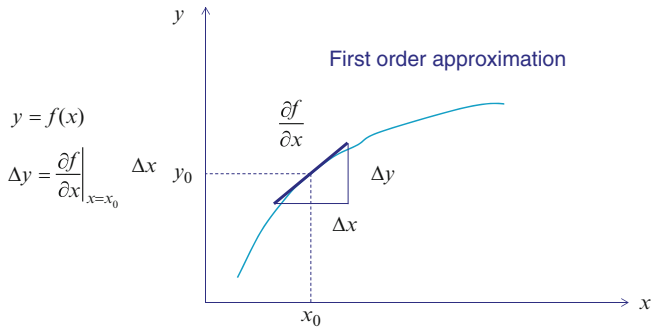

Fig. 5.1 First order approximation to propagate uncertainty

5.3.2 Second Stage: PolyMAX Applied to the MLE Synthesized Model

Despite the nice statistical properties of MLE, some hurdles still need to be taken to make it a practical method compatible with the "state-of-the-use" in modal parameter estimation:

- Often a stabilization diagram is used to distinguish real poles from numerical poles [13]. Due to the iterative character of the method, it is rather time-consuming to construct an MLE stabilization diagram. Also the resulting diagram is not so easy to interpret as in case of PolyMAX [14].
- The FRF model considered in MLE is a common-denominator model, which is not fully compatible to a poly-reference modal model.

Therefore, it is proposed to apply MLE using a fixed model order (i.e. without constructing a stabilization diagram) and post-process the synthesized FRFs using the PolyMAX method [15]. The idea is that MLE removes the noise from the data and that PolyMAX will then allow selecting the physical poles by means of the stabilization diagram.

5.3.3 Third Stage: Estimation of the Confidence Bounds from an MLE Modal Model Formulation

After having identified a modal model Eq. (5.8), the confidence bounds on the modal parameter estimates still have to be computed. The basic principle is that the uncertainty on the measurement data $\sigma_{H_{oi}}$ is propagated to an uncertainty on the modal parameter estimates (standard deviation of eigenfrequency σ_{ω_i} and damping ratio σ_{ξ_i}:

$$\sigma_{H_{oi}} \rightarrow \sigma_{\omega_i}, \sigma_{\xi_i} \tag{5.12}$$

The (analytical) relation between the covariances of the FRFs and the covariances of the MLE model parameters is given by the Jacobian matrix evaluated during the last iteration step of the Gauss-Newton algorithm. The confidence bounds on frequency and damping estimates can then be calculated from the covariances of the MLE model parameters [16].

The principle is illustrated in Fig. 5.1. The modal parameters are a function of the measured FRFs. Therefore, the derivative (Jacobian) of these functions can be used to calculate confidence bounds on the modal parameters based on FRF uncertainty.

In the particular case of PolyMAX Plus, the MLE cost function like in Eq. (5.10) is formulated, but the FRF model is a modal model like in Eq. (5.8). Also, the second stage modal parameters are retained and no iterative process is started, but only the Jacobian is calculated in order to calculate the covariances of the modal parameters. Details on the specific implementation for the MLE method applied to a modal model can be found in [10].

5.4 Numerical and Measurement Examples

5.4.1 Acoustic Modal Analysis Measurement Example

The passenger cavity of an airplane has been measured using four loudspeakers as exciters and a grid of microphones that measured a total of 240 locations in multiple runs. The data has been measured very long time ago and unfortunately, only FRFs have been retrieved from the historical database. Nevertheless it remains an interesting measurement because of the many exciters that have been used Eq. (5.4) and the fact that it is an acoustic modal analysis example with highly-damped modes and a large number of microphones. It is beyond the scope of this paper to go in full detail on the specifics of this example, but the idea is to illustrate the use of smoothed residual errors to get an estimate on the data uncertainty (Sect. 5.2). The MLE method was applied to the 240×4 FRF matrix and the curve-fitting results are represented in Fig. 5.2. The blue line indicate the estimated standard deviation $\sigma_{H_{oi}}$. The FRF at the right figure looks noisier, which is confirmed by the higher standard deviation. Also at the left, there is an area around 70 Hz where the FRF is noisy, the data is not very well fitted and the standard deviation goes up.

5.4.2 Numerical Example: Lightly-Damped Structure with Closely-Spaced Modes

In this section, a numerical example consisting of 23 outputs, 4 inputs and 12 lightly-damped modes between 5 and 65 Hz (see first two columns of Table 5.2) is used to validate the different FRF variance estimation approaches outlined in Sect. 5.2. Some of the modes are closely-spaced in frequency. White noise (5 %) has been added to all outputs (i.e. satisfying the H1 assumptions). In this simulation example, pseudo-random excitation [17] was used with seven repetitions of each realization (three delay blocks and four acquisition blocks). The delay blocks are used to let the transients decay and to avoid leakage errors. A total of 25 realizations have been applied, leading to $25 \times 4 = 100$ averages. This simulation has been performed for different properties of the four pseudo-random input signals:

- Uncorrelated with equal power.
- Uncorrelated with non-equal power.
- "Mildly" correlated.
- "Heavily" correlated.

The corresponding input spectrum matrices S_{uu} are represented in the second row of Table 5.1. Also the condition numbers of these matrices with respect to inversion are provided in the table (third row). The condition number is the ratio of the largest singular value to the smallest. Large condition numbers indicate a nearly singular matrix.

For each case, the FRF variance was estimated using three different approaches:

- According to Eq. (5.5) using the full input spectrum matrix.
- According to Eq. (5.5) using a diagonal input spectrum matrix.
- According to Eq. (5.7) without using input spectra.

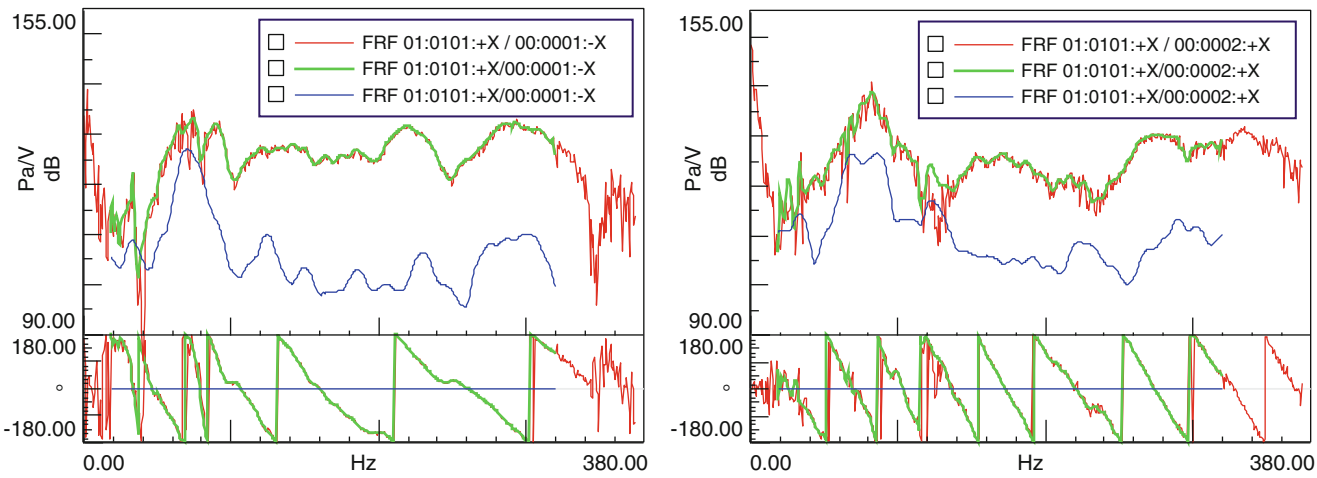

Fig. 5.2 Acoustic FRFs: measurements, MLE fit, standard deviation based on the residual-error approach

Table 5.1 Accuracy of pragmatic approaches to estimate the FRF standard deviation as a function of input correlations and power spectra

Input correlation/power spectra	Uncorrelated/equal power spectra	Uncorrelated/non-equal power spectra (Fig. 5.3)	"Mildly" correlated (Fig. 5.4)	"Heavily" correlated (Fig. 5.5)
Input spectrum matrix	$\begin{bmatrix} 1 & 0 & 0 & 0 \\ 0 & 1 & 0 & 0 \\ 0 & 0 & 1 & 0 \\ 0 & 0 & 0 & 1 \end{bmatrix}$	$\begin{bmatrix} 1 & 0 & 0 & 0 \\ 0 & 4 & 0 & 0 \\ 0 & 0 & 9 & 0 \\ 0 & 0 & 0 & 16 \end{bmatrix}$	$\begin{bmatrix} 1 & 1 & 0.5 & 0.5 \\ 1 & 5 & 1.5 & 1.5 \\ 0.5 & 1.5 & 9.5 & 3.5 \\ 0.5 & 1.5 & 3.5 & 17.5 \end{bmatrix}$	$\begin{bmatrix} 1 & 2 & 3 & 4 \\ 2 & 8 & 12 & 16 \\ 3 & 12 & 27 & 36 \\ 4 & 16 & 36 & 64 \end{bmatrix}$
Condition number of input spectrum matrix	1	16	25	196
Average error on FRF std estimate using input power spectra only	1 %	1 %	4 %	78 %
Average error on FRF std estimate without using input spectra	1 %	91 %	135 %	558 %

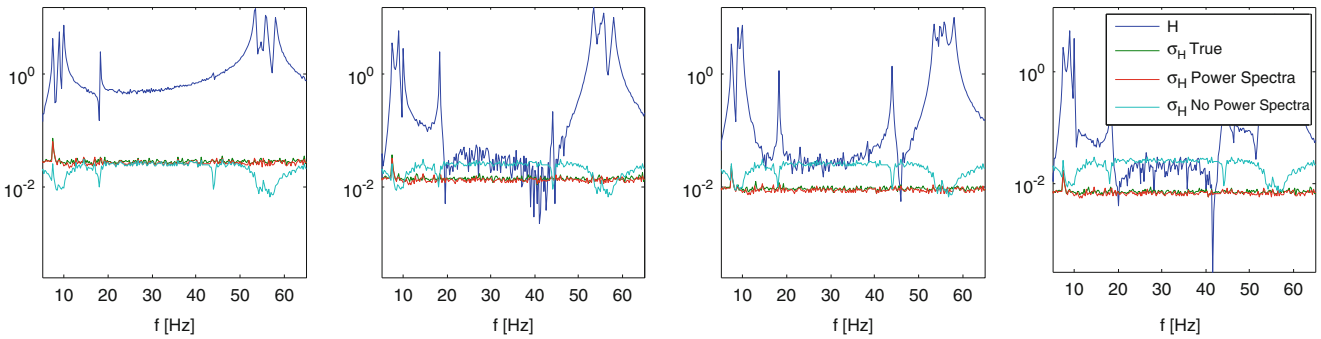

Fig. 5.3 Uncorrelated inputs with non-equal power: one row of the FRF matrix and three different approaches to estimate the standard deviation

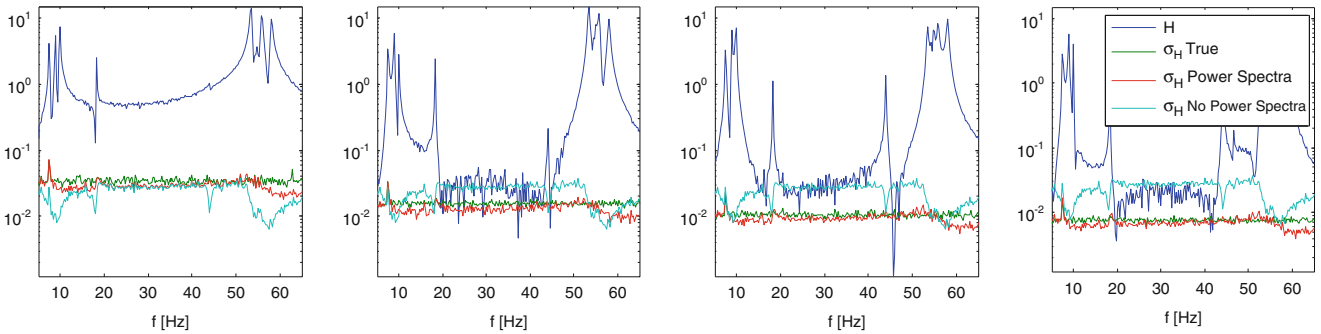

Fig. 5.4 "Mildly" correlated inputs: one row of the FRF matrix and three different approaches to estimate the standard deviation

The results are represented in Table 5.1, Figs. 5.3, 5.4, and 5.5. The error has been calculated wrt. the first approach Eq. (5.5) which is considered to be the "true" one. For the case with uncorrelated inputs with equal power, all three approaches agree almost perfectly (1 % deviation). This is not surprising since the assumptions that need to be made in the pragmatic approaches are satisfied with a diagonal input spectrum matrix with equal elements on the diagonal. In case of uncorrelated inputs with non-equal power, the last approach shows large estimation errors on the FRF standard deviations. If the input power spectra differ a lot, it is important to include them in the estimate. In case of "mildly" correlated inputs, the approach that uses a diagonal input spectrum matrix (i.e. neglecting the correlations), still provides satisfactory results (4 % error). In case of "heavily" correlated inputs, large errors are observed using the pragmatic approaches.

Finally, the PolyMAX Plus method was applied to the case with uncorrelated inputs with equal power. The results are represented in Table 5.2. In the PolyMAX Plus method, the residual error approach was used to estimate the FRF standard deviations. These estimates are compared to the "true" estimates in Fig. 5.6. Overall, the residual error follows the true standard deviations, except at the resonances were the FRF uncertainty is overestimated due to fitting errors of the FRF data which are included in the residual errors obviously. This can be improved by using an MLE fit after some iterations rather than the fit based on the initial values of the FRF model (LSCF method). The colorbars in Table 5.2 are scaled to the maximum

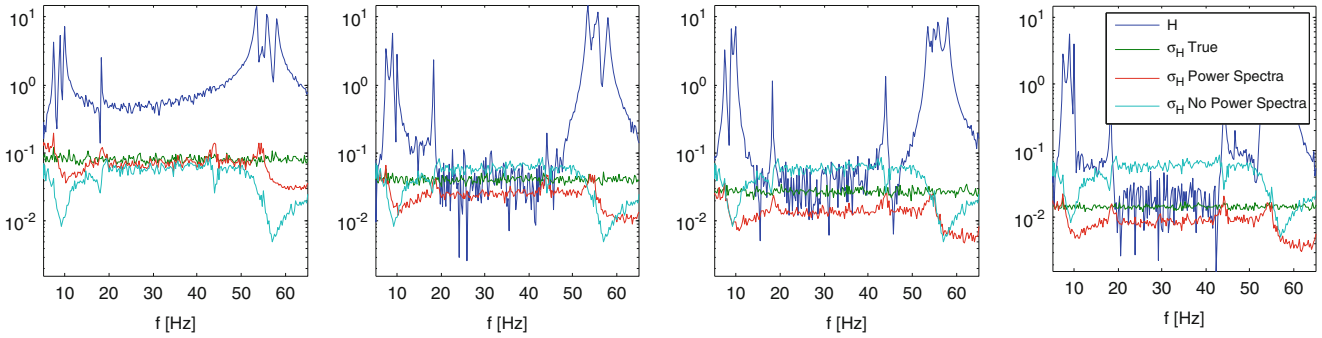

Fig. 5.5 "Heavily" correlated inputs: one row of the FRF matrix and three different approaches to estimate the standard deviation

Table 5.2 True and estimated (using PolyMAX Plus) modal parameters with relative uncertainties of the different modes represented by the colorbars: s_f and s_xi represent the relative standard deviations on the frequencies and damping ratios. The uncertainties have been calculated using two different data standard deviation estimates: using the "true" std (5) and the residual error approach

True		PolyMAX Plus					
				True sigma		Residual Error	
f [Hz]	xi [%]	f [Hz]	xi [%]	s_f [Hz]	s_xi [%]	s_f [Hz]	s_xi [%]
7.58	0.41	7.59	0.43	0.0001	0.0009	0.0002	0.0027
8.95	0.65	8.95	0.65	0.0000	0.0003	0.0004	0.0050
9.92	0.67	9.93	0.70	0.0000	0.0002	0.0007	0.0066
10.03	0.68	10.03	0.69	0.0000	0.0002	0.0007	0.0069
18.24	0.19	18.24	0.19	0.0000	0.0002	0.0001	0.0004
44.04	0.14	44.04	0.14	0.0000	0.0000	0.0000	0.0001
46.69	0.06	46.68	0.05	0.0005	0.0010	0.0029	0.0062
53.43	0.34	53.43	0.34	0.0000	0.0000	0.0001	0.0002
54.39	0.14	54.39	0.14	0.0001	0.0001	0.0005	0.0009
54.84	0.30	54.84	0.30	0.0000	0.0000	0.0001	0.0002
55.83	0.38	55.83	0.38	0.0000	0.0000	0.0001	0.0002
58.00	0.37	58.00	0.37	0.0000	0.0000	0.0000	0.0000

across each column, but it is important to note that the uncertainties calculated using the residual error approach are much larger (the colorbars should in fact be more than 6× longer). It is also clear that the modes around 9–10 Hz get relatively a much higher uncertainties in the residual-error method. This is due to the large fitting errors in this region (see Fig. 5.6).

5.4.3 Multiple-Input In-Flight Measurement Data

In this section, a similar study as in Sect. 5.4.2 is performed, but using real measurement data. It concerns a typically noisy in-flight FRF measurement where two exciters have been used. The large noise levels originate from the turbulences and harsh measurement conditions during flight. Note that for confidentiality reasons, the frequency values have been omitted. Again three approaches to estimate the variance of the FRFs have been compared. Figure 5.7 shows the measured power and cross spectra. It can be seen that both power spectra are quite close in amplitude and that the cross spectrum is significantly lower. This provides the justification for using the pragmatic approach to estimate the FRF variances in case of uncorrelated inputs with equal power. Figure 5.8 compares the three different estimates and it can be concluded that even with reduced information (only using input power spectra or even not using any power/cross input spectrum), very reasonable variance estimates are obtained.

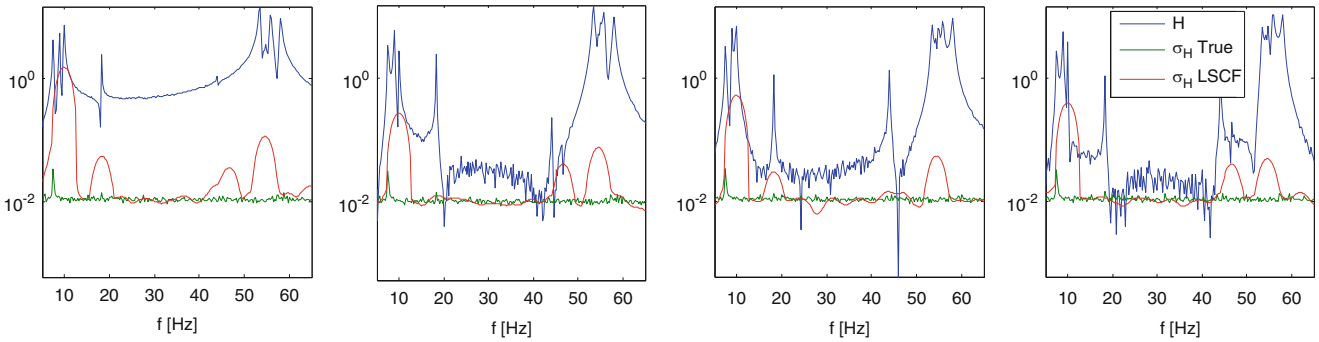

Fig. 5.6 Uncorrelated inputs with equal power: one row of the FRF matrix and two different approaches to estimate the standard deviation: the "true" one (5) and the one based on the residual error approach

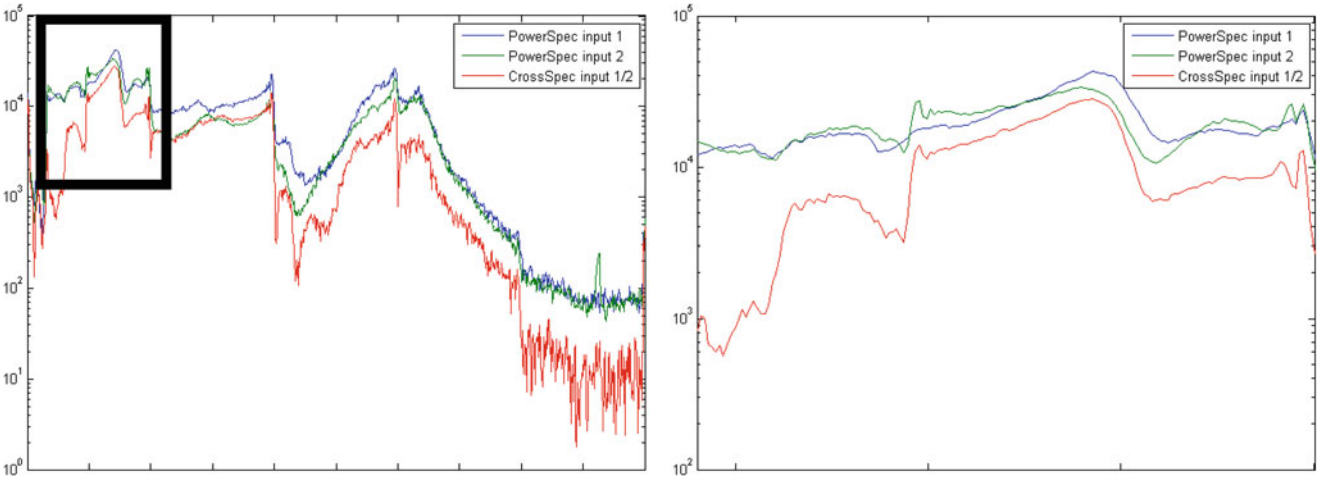

Fig. 5.7 Two power spectra and the cross spectrum between two excitation forces applied to an aircraft during flight. A zoom into the useful frequency range is provided in the right figure

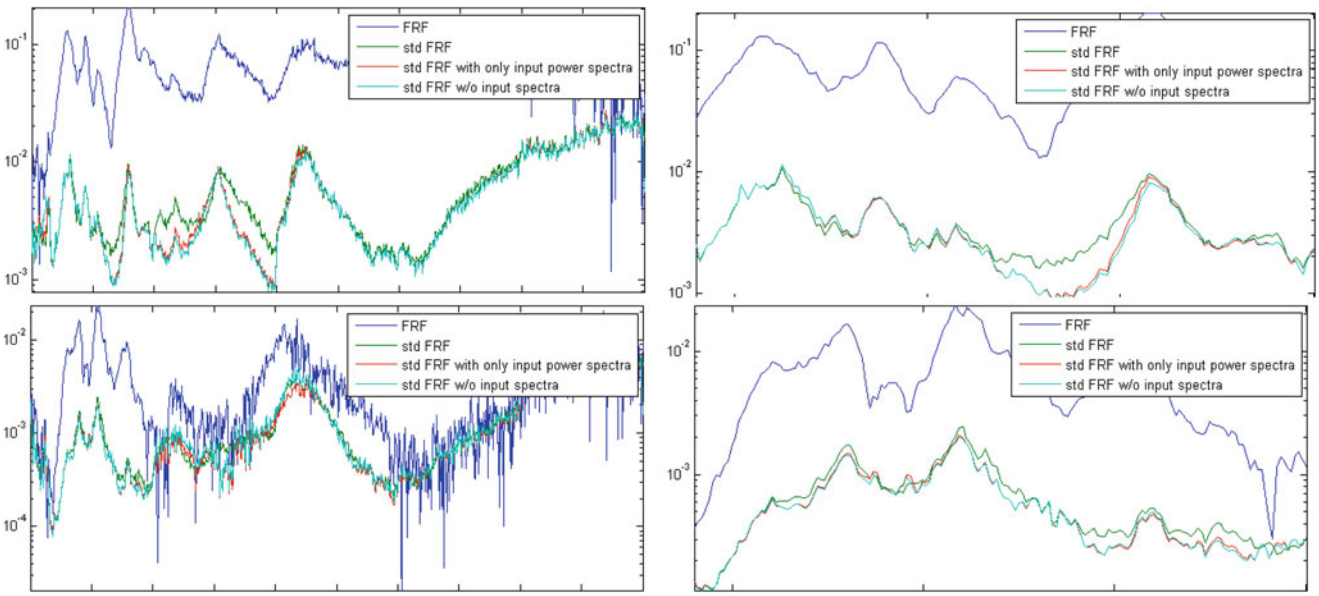

Fig. 5.8 In-flight FRFs and three different approaches to estimate the standard deviation. (*Top*) high quality FRF; (*Bottom*) noisier FRF. (*Left*) full frequency range; (*Right*) Zoom

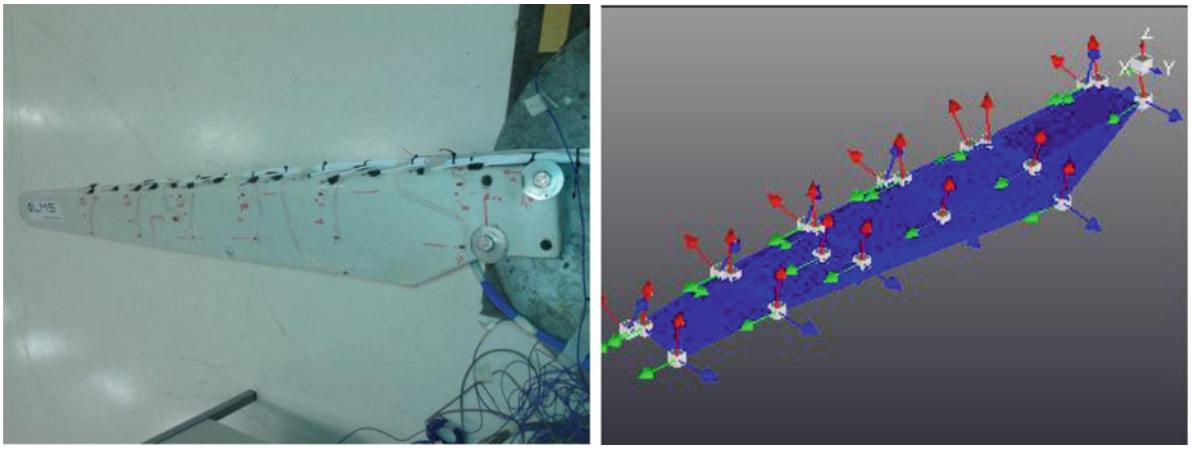

Fig. 5.9 (*Left*) Test set-up: clamped composite small wind turbine blade; (*Right*) sensor locations

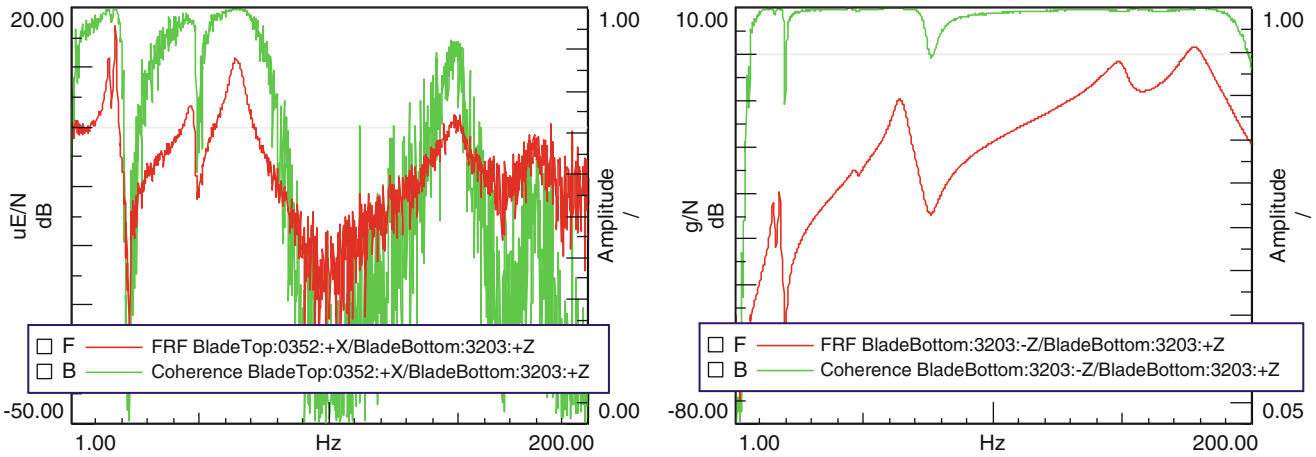

Fig. 5.10 Typical FRF and coherence function: (*Left*) strain gauge response signal; (*Right*) acceleration response signal

5.4.4 Comparison of Strain Gauges and Accelerometers

In this section, measurement results from a clamped composite small wind turbine blade will be shown (Fig. 5.9). More details on the use of strain gauge data for experimental modal analysis can be found in [18]. The interest to take a look at these data in the context of this paper is to study the impact of the sensor measurement noise on the estimated modal parameters. The blade response to impact excitation was recorded by a number of strain gauges and accelerometers distributed along the structure. From Fig. 5.10, the quality differences between a strain and an acceleration FRF are clear. At higher frequencies (>200 Hz), the coherence values of the strain measurements continue to decrease. Although both datasets yield comparable and reliable modal parameters, it is clear that the uncertainty bounds on the eigenfrequencies and damping ratios estimated with strain gauges are considerably higher than the bounds obtained from acceleration measurement (Table 5.3).

5.5 Conclusions

The potential of structural dynamics test and analysis methods for addressing a noise and vibration design assessment or design optimisation, depends largely on the confidence that one can have in the results. In other words, the results must be accurate, characteristic for the actual problem (and not be the result of testing artefacts) and representative for the actual behaviour of the investigated structure(s). This paper discussed the propagation of measurement noise into uncertainty on the estimated modal parameters using the PolyMAX Plus method. This paper discussed different approaches to estimate the

Table 5.3 Small wind turbine blade modal parameters obtained using PolyMAX Plus from both strain FRF and acceleration FRF measurements. The s_f/f and s_xi/xi represent the relative standard deviations on the frequencies and damping ratios

Mode	Strain FRFs				Accel FRFs			
	f [Hz]	s_f / f	xi [%]	s_xi / xi	f [Hz]	s_f / f	xi [%]	s_xi / xi
1	15.35	0.02%	2.81%	0.74%	15.33	0.01%	3.01%	0.43%
2	17.70	0.01%	1.72%	0.50%	17.69	0.01%	1.67%	0.36%
3	47.36	0.01%	2.72%	0.45%	46.98	0.01%	3.59%	0.31%
4	64.16	0.01%	3.55%	0.26%	64.00	0.00%	3.77%	0.11%
5	66.51	0.05%	2.07%	2.53%	66.25	0.01%	3.49%	0.37%
6	148.96	0.01%	3.14%	0.21%	149.83	0.00%	2.28%	0.09%
7	178.53	0.01%	3.13%	0.32%	178.94	0.01%	3.20%	0.17%

variance on the FRFs even for cases where no detailed noise information is available. The basic concepts of PolyMAX Plus method and its relation to Maximum Likelihood Estimation have been highlighted. Finally some numerical simulation and real measurements examples have been discussed.

References

1. Van der Auweraer H, Donders S, Peeters B (2005) Importance of uncertainty in identifying and using modal models. Proceedings of the International Symposium on Managing Uncertainty in Noise Measurement and Prediction, Le Mans, France
2. Govers Y, Link M (2010) Stochastic model updating: covariance matrix adjustment from uncertain experimental modal data. Mechanical Systems and Signal Processing 24(3):696–706
3. Govers Y, Link M (2012) Using stochastic experimental modal data for identifying stochastic finite element parameters of the AIRMOD benchmark structure. Proceedings of the ISMA 2012, Leuven, Belgium
4. Ewins DJ (2000) Modal testing: theory, practice and applications, 2nd edn. Research Studies Press, Baldock, UK
5. Heylen W, Lammens S, Sas P (2013) Modal analysis theory and testing. Department of Mechanical Engineering, Katholieke Universiteit Leuven, Leuven
6. Bendat J, Piersol A (1971) Random data: analysis and measurement procedures. Wiley, New York
7. Pintelon R, Schoukens J (2001) System identification: a frequency domain approach. IEEE, New York
8. El-kafafy M (2013) Design and validation of improved modal parameter estimators, PhD thesis, VUB, Brussels, Belgium
9. El-kafafy M, Guillaume P, Peeters B (2013) Modal parameter estimation by combining stochastic and deterministic frequency-domain approaches. Mechanical System and signal Processing 35(1–2):52–68
10. El-kafafy M, De Troyer T, Peeters B, Guillaume P (2013) Fast maximum-likelihood identification of modal parameters with uncertainty intervals: a modal model-based formulation. Mech Syst Signal Process 37:422–439
11. Peeters B, El-kafafy M,Guillaume P (2012) The new PolyMAX Plus method: confident modal parameter estimation even in very noisy cases. Proceedings of the ISMA 2012, Leuven, Belgium
12. Guillaume P, Verboven P, Vanlanduit S (1998) Frequency-domain maximum likelihood identification of modal parameters with confidence intervals. Proceedings of the ISMA 23, Leuven, Belgium
13. Van der Auweraer H, Peeters B (2004) Discriminating physical poles from mathematical poles in high order systems: use and automation of the stabilization diagram. Proceedings of the IMTC 2004, the IEEE Instrumentation and Measurement Technology Conference, Como, Italy
14. El-kafafy M, Guillaume P, Peeters B, Marra F, Coppotelli G, Advanced frequency-domain modal analysis for dealing with measurement noise and parameter uncertainty. Proceedings of the IMAC 30, Jacksonville FL, USA
15. Peeters B, Van der Auweraer H, Guillaume P, Leuridan J (2004) The PolyMAX frequency-domain method: a new standard for modal parameter estimation? Shock and Vibration 11:395–409
16. Pintelon R, Guillaume P, Schoukens J (2007) Uncertainty calculation in (operational) modal analysis. Mechanical System and Signal Processing 21(6):2359–2373
17. Guillaume P, Verboven P, Vanlanduit S, Parloo E (2001) Multisine excitations: new developments and applications in modal analysis. Proceedings of the IMAC 19, Kissimmee, FL
18. Santos F, Peeters B, Menchicchi M, Lau J, Gielen L, Desmet W, Goes L (2014) Strain-based dynamic measurements and modal testing. Proceedings of the IMAC 32, Orlando, FL, USA